https://doi.org/10.5194/egusphere-2025-15
Preprint. Discussion started: 31 March 2025

Widespread stratospheric intrusion influence on summer ozone pollution over China revealed by multi-site ozonesonde, ground-based measurement and fully-validated reanalysis

Zhiheng Liao[1], Jinqiang Zhang[2], Meng Gao[3], Zhiqiang Ma[1]

1 Institute of Urban Meteorology, China Meteorological Administration, Beijing, China
2 Key Laboratory of Middle Atmosphere and Global Environment Observation, Institute of Atmospheric Physics, Chinese Academy of Sciences, Beijing, China
3 Department of Geography, Hong Kong Baptist University, Hong Kong SAR, China

Correspondence: Z. Ma (zqma@ium.cn)

Abstract

Understanding stratospheric intrusion (SI) is crucial for elucidating atmospheric complexities and improving strategies to mitigate surface ozone (O_3) pollution. This study investigates a deep trough-induced SI event in China from June 10 to 13, 2013, based on ozonesondes from Beijing, Changchun, and Hong Kong, nationwide ground-based measurements, and fully-validated reanalysis products. Ozonesondes from Beijing indicated notable high-level secondary ozone peaks (> 400 ppbv) since June 11. Tropospheric sub-high ozone layers were observed in Changchun on June 12 (> 120 ppbv) and Hong Kong on June 13 (> 80 ppbv). Nationwide surface ozone measurements recorded severe ozone pollution (> 100 ppbv) from western plateaus to eastern plains over China. Together, these observations suggest a widespread influence of stratospheric ozone intrusion. Further, the ozonesonde-validated EAC4 reanalysis reproduced the fine-scale SI structure (O_3-rich "tongue"), in turn well explaining the secondary ozone peaks and sub-high ozone layers in ozonesonde observations. The O_3-rich "tongue" swept through the Tibetan Plateau on June 10, triggering extreme ozone pollution with a stratospheric ozone contribution up to 30 ppbv (>30 %). With the trough's eastward movement, the O_3-rich "tongue" penetrated into the lower troposphere of eastern China, and then be entrained into the surface layer, exacerbating severe ozone pollution occurred in the Northern China Plain on June 13, with a stratospheric ozone contribution of 3–15 ppbv (2–10 %). This research underscores the importance of multi-site ozonesondes in understanding stratospheric ozone intrusions and the potential of the publicly available EAC4 reanalysis in multiyear SI analyses.

Keywords: stratospheric intrusion; secondary ozone peak; surface ozone pollution; high-level trough; contribution

1 Introduction

Surface ozone (O_3) poses significant risks to public health and ecosystem productivity due to its strong oxidative properties (Monks et al., 2015). While O_3 in the lower atmosphere is predominantly produced through photochemical reactions, stratospheric intrusion (SI)—the process where O_3-rich air masses from the stratosphere descend to the lower troposphere—can also increase surface O_3 concentrations in certain regions (Akritidis et al., 2018; Skerlak et al., 2019; Dreessen, 2019). The natural SI processes complicate efforts to manage and reduce anthropogenic O_3 pollution. Therefore, understanding how SI affects surface O_3 is crucial for improving strategies to mitigate O_3 pollution.

SI is a key component of extratropical weather processes, and detecting SI events has been a major scientific concern since the 1970s (Appenzeller and Davies, 1992; Stohl et al., 2003; Hocking et al., 2007; Lin et al., 2016; Lin et al., 2021; Liu et al., 2024). Numerous evidences have shown that surface O_3 concentrations can episodically rise during the SI event (Cristofanelli et al., 2010; Langford et al., 2012; Yates et al., 2013; Lin et al., 2015;

https://doi.org/10.5194/egusphere-2025-15
Preprint. Discussion started: 31 March 2025

Dreessen, 2019; Ou-Yang et al., 2022; Chen et al., 2023; Chen et al., 2024). However, the detailed structure of stratospheric ozone intrusion into the surface layer remains poorly understood due to limited ozonesonde measurements (Chen et al., 2011; Zhao et al., 2021; Hong et al., 2024). Consequently, the stratospheric intrusion contribution to surface ozone has long been a topic of much debate over the past few decades (Stohl et al., 2003; Yang et al., 2022; Zheng et al., 2024). Up to now, much of the understanding of SI and its contribution to surface O_3 pollution comes from satellite observations, atmospheric reanalysis, and model simulations (Li et al., 2015; Lu et al., 2019; Wang et al., 2020a; Zhao et al., 2021; Zhang et al., 2022; Chen et al., 2023; Chang et al., 2023; Hong et al., 2024; Luo et al., 2024; Zhao et al., 2024; Zhu et al., 2024; Meng et al., 2024; Knowland et al., 2017). Although open-source products and custom model simulations show a certain ability in capturing the stratospheric ozone intrusion and even quantifying the stratospheric intrusion contribution, their results still possess large uncertainties due to a common dearth of validation against with vertical O_3 measurements. Besides, recent attempts to quantify stratospheric influences using ground-based chemical tracers also have embedded uncertainties because little is known about the SI structure aloft from the ground-based measurements alone (Zheng et al., 2024). Opposite conclusions were even drawn from different chemical tracers. For example, an isotopic (^{35}S) chemical tracer study (Lin et al., 2021) revealed a west-high-east-low stratospheric intrusion contribution over China, whereas an O_3-CO chemical tracer study (Chen et al., 2024) suggested an inverse distribution. The lack of consensus lead to a significant cognitive confusion, emphasizing the urgent need of direct ozonesonde observations to refine the fundamental understanding of stratospheric ozone intrusion and its contribution to surface ozone pollution.

This study focuses on a typical SI event associated with an upper-level trough observed over China during June 10–13, 2013, to investigate its influence on summer ozone pollution. During this event, nationwide air quality measurements performed by the China National Environmental Monitoring Centre recorded severe surface ozone pollution (exceeding 100 ppbv) from the high-elevation Tibetan Plateau to the low-altitude eastern China. We conducted intensive ozonesonde observations (daily resolution) in Beijing and Changchun, and collected routine ozonesonde (weekly resolution) in Hong Kong. Through detailed analysis of multi-site ozonesondes, ground-based measurements, and fully-validated reanalysis products (*Datasets*) in this SI event, this study aims to 1) characterize the spatial and temporal behavior of upper-level trough-induced stratospheric ozone intrusion, 2) quantify its contribution to surface ozone pollution, and 3) elucidate the underlying dynamical transport mechanisms.

2 Datasets

2.1 Ozonesonde observation

Ozonesondes provide a detailed vertical ozone profiles and thus are an important tool for quantifying the vertical distribution of ozone and therefore have been useful in validating satellite retrievals of ozone and atmospheric ozone reanalysis products. In China, ozonesondes, along with radiosondes, were routinely launched weekly in Beijing (116.47 °E, 39.80 °N; 33 m above mean sea level (MSL)) and Hong Kong (114.17 °E, 22.31 °N; 66 m above MSL). During June 2013, an intensive ozonesonde launch experiment was held in Beijing and Changchun (125.20 °E, 43.90 °N; 237 m above MSL), with consecutive launches from June 10–13 (Zhang et al., 2013). These sondes were launched around 13:30 China Standard Time (CST), providing high-resolution profiles of ozone partial pressure, atmospheric pressure, temperature, and humidity from the surface up to approximately 35 km (Zhang et al., 2021; Liao et al., 2024). For this study, data from nine ozonesonde observations were analyzed to examine stratospheric ozone intrusion during June 10–13, 2013, including four consecutive days in Beijing and Changchun, and a single launch on June 13 in Hong Kong.

2.2 Atmospheric reanalysis data

https://doi.org/10.5194/egusphere-2025-15
Preprint. Discussion started: 31 March 2025

ERA5, the fifth-generation ECMWF (European Centre for Medium-Range Weather Forecasts) global reanalysis, offers a comprehensive dataset at a spatial resolution of 0.25 ° × 0.25 ° and a temporal resolution of 1 hour for climate and weather analysis (Hersbach et al., 2020). It integrates model data with observations using four-dimensional variational assimilation (4D-Var) in ECMWF's Integrated Forecast System (IFS). This study utilized ERA5 data, including geopotential height, potential vorticity, vertical velocity, and wind fields, to describe the synoptic conditions during the stratospheric intrusion event.

EAC4 (ECMWF Atmospheric Composition Reanalysis 4) represents the fourth generation of ECMWF's atmospheric composition reanalysis, with a spatial resolution of 0.75 ° × 0.75 ° and a temporal resolution of 3 hours (Inness et al., 2019). EAC4 assimilates data from various satellite sources, including total column ozone from the Ozone Monitoring Instrument (OMI) and Global Ozone Monitoring Experiment-2 (GOME-2) on Metop satellites, profile data from the Microwave Limb Sounder (MLS), and partial columns from Solar Backscatter Ultra-Violet (SBUV/2) and Ozone Mapping and Profiler Suite (OMPS). The IFS used in EAC4 incorporates an extended version of the Carbon Bond 2005 (CB05) chemical mechanism, which includes 126 tropospheric reactions. EAC4 provides both ozone (O_3) and stratospheric ozone tracer (O_3S, O_3 originating from the stratosphere). This study employed both O_3 and O_3S to characterize the three-dimensional structure of stratospheric ozone intrusion.

2.3 Auxiliary data

Additional data sources included ground-based ozone measurements from the China National Air Quality Monitoring Network, satellite cloud images from the Moderate Resolution Imaging Spectroradiometer (MODIS), Level-3 ozone profile products from the Atmospheric Infrared Sounder (AIRS), and ozone reanalysis products from the Modern-Era Retrospective Analysis for Research and Applications, Version 2 (MERRA2). Hourly surface ozone concentrations from 76 cities in China during June 10–13, 2013, were used to assess nationwide ozone pollution during the stratospheric intrusion event. MODIS satellite cloud images illustrated the weather conditions, while AIRS and MERRA2 ozone products served as alternative references to EAC4 data.

3 Results

3.1 Ozonesonde evidence of stratospheric ozone intrusion

Fig. 1 illustrates the evolution of the high-level trough event from June 10 to 13, 2013. On June 10, the upper-level trough extended from the Mongolian Plateau towards the Tibetan Plateau. By June 11, the trough had moved eastward and deepened into a "V-shaped" structure between 90°E and 120°E, causing an extremely distorted westerly jet and strong northerlies at the western flank of the trough. On this day, the emerged 1.5 PVU potential vorticity contours at 400 hPa provide convincing evidence for a deep stratospheric intrusion. On June 12, the "V-shaped" trough persisted at 200 hPa. By June 13, the high-level trough had weakened to be a shallow structure over the North China Plain (NCP). Three-dimensional dynamics associated with upper-level troughs involves stratospheric dry intrusion (SDI) and warm conveyor belts (WCB) airstreams (Browning and Roberts, 1994; Browning, 1997). The SDI originates in the lower stratosphere on the cold side of the trough (west of the trough axis) and descends behind the cold front, while the WCB originates in the warm sector of the trough (east of the trough axis), ascending rapidly to the mid- and upper troposphere. During this event, these contrasting airstreams led to significantly different weather at the two sides of the trough, with cloudy weather in the WCB zone (east) and clear weather in the SDI zone (west). There appeared an obvious transition from cloudy to clear weather in the eastern China with the eastward movement of upper-level trough. On June 13, China, excluding the northeast and eastern coastal regions, experienced clear weather.

https://doi.org/10.5194/egusphere-2025-15
Preprint. Discussion started: 31 March 2025

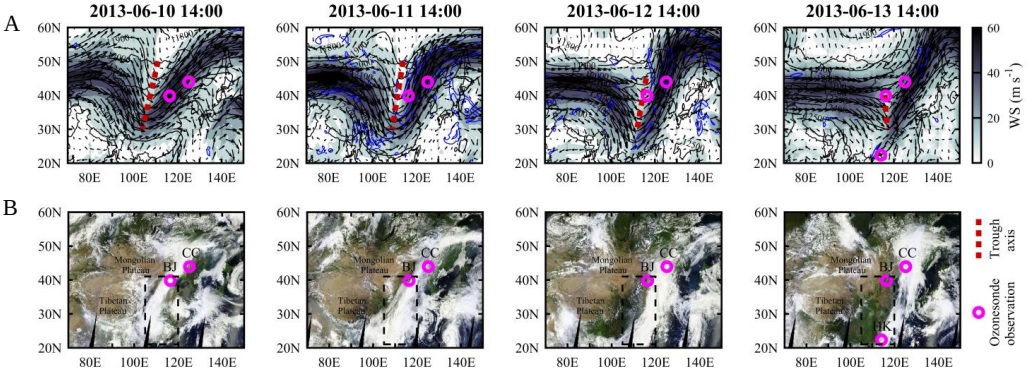

Fig. 1. (A) Horizontal distribution of geopotential height (black contours, units in gpm), wind speed (shading, units in m s^{-1}), and wind direction (arrows) at 200 hPa, and potential vorticity (blue contours, 1.5 PVU) at 400 hPa. (B) MODIS satellite cloud images with the dashed box marking eastern China (105 °E–120 °E, 21 °N–41 °N). Red dot lines denote the axis of upper-level trough. Magenta circles mark the available ozonesondes at different sites (BJ: Beijing, CC: Changchun, and HK: Hong Kong) on different days.

Stratospheric ozone intrusion remains uncertain due to sharp spatial gradients and high variability in ozone concentrations caused by competing transport and mixing processes near the extratropical tropopause (Skerlak et al., 2019). The continuous and multi-site ozonesondes provided a unique opportunity to characterize stratospheric ozone intrusion linked to upper-level trough (Fig. 2). On June 10, before the trough arrived, Beijing was influenced by WCB airstreams, showing high humidity (RH > 60%) in the upper troposphere. By June 11, Beijing was near the trough axis, and the O_3-rich SDI airstream began to affect the upper atmosphere, creating a secondary ozone peak (~400 ppbv at 9.5 km height) above the rapidly descended thermal tropopause (which dropped from 10.5 km on June 10 to 8.2 km on June 11). Besides, stratospheric intrusion led to a quick drop in relative humidity from 70% on June 10 to below 25 % on June 11 in the upper troposphere of Beijing. On June 12 and 13, the secondary ozone peaks continued to be observed over Beijing, with peak concentrations rising to 650 ppbv by June 13, but the altitude of these peaks gradually increased up to 13.6 km by June 13 with the elevation of thermal tropopause. High-level secondary ozone peaks are a characteristic O_3-profile structure associated with tropospheric folding, a major form of SI in the extratropical region (Lemoine, 2004; Hwang et al., 2007; 2011; Chen et al., 2011; Ojha et al., 2017; Bartusek et al., 2023). Unlike that in Beijing, the sonde-based O_3 profiles in Changchun showed high-level secondary ozone peak only in June 13, when high-level trough moved eastward to affect Changchun. However, sub-high ozone layer (> 120 ppbv) appeared in the middle troposphere (4.2–8.1 km height) in advance on June 12, accompanied by extremely low relative humidity. Similar sub-high ozone layer (> 80 ppbv) also occurred in the lower troposphere (3.5–6.0 km height) of Hong Kong on June 13. These high-ozone and low-humidity air masses in the troposphere reflect obvious stratospheric origin, suggesting a widespread SI influence during this deep trough process.

https://doi.org/10.5194/egusphere-2025-15
Preprint. Discussion started: 31 March 2025

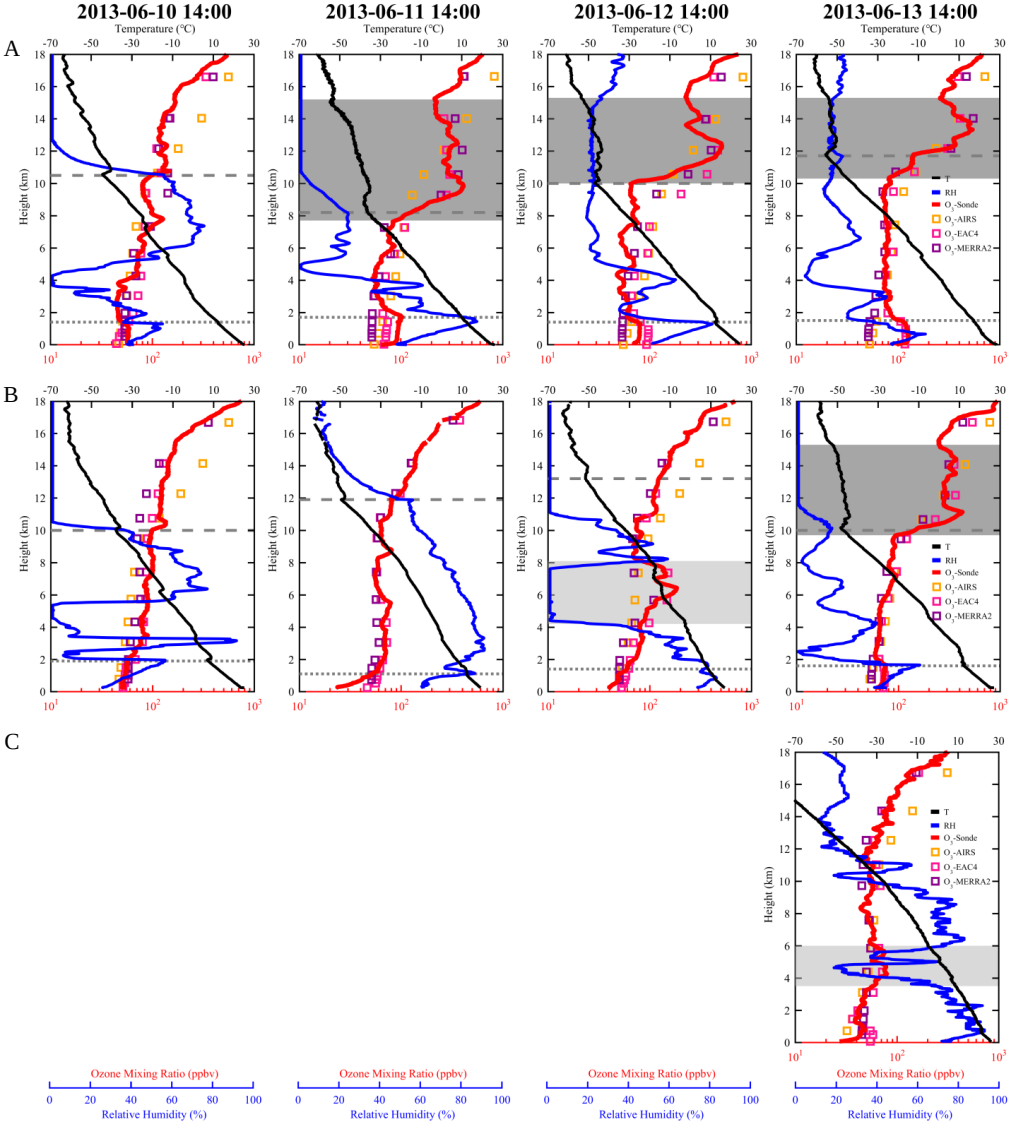

Fig. 2. Ozone vertical distribution over (A) Beijing, (B) Changchun, and (C) Hong Kong derived from ozonesonde and other data sources (including AIRS satellite observation, EAC4 and MERRA2 reanalysis) during 10–13 June 2013. Black and blue lines denote the sonde-based temperature (T) and relative humidity (RH) profiles, respectively. Gray dashed lines represent the thermal tropopause height, and gray dot lines indicate the boundary layer top height. High-level secondary ozone peaks are shaded heavy gray, and SI-induced O_3-rich layer in the troposphere is shaded light gray.

3.2 Three-dimensional structure of stratospheric ozone intrusion

The multi-site ozonesonde observations only provide a snapshot of stratospheric ozone intrusion at its influence scale. To further visualize the three-dimensional structure of the stratospheric ozone intrusion, we introduced the

https://doi.org/10.5194/egusphere-2025-15
Preprint. Discussion started: 31 March 2025

commonly-used large-scale ozone products, including AIRS satellite observation, MERRA2 and EAC4 reanalysis (Li et al., 2015; Knowland et al., 2017; Akritidis et al., 2018). Before utilizing these large-scale ozone products, we validated them against our ozonesonde observations. As shown in Fig. 2, AIRS satellite observation missed the upper-level secondary ozone peaks and the boundary-layer ozone enhancements. MERRA2 reanalysis captured the secondary ozone peaks but still showed large negative biases to the observed boundary-layer ozone enhancements. In contrast, EAC4 reanalysis reproduced well the major features of the ozone vertical distribution, including upper-level secondary ozone peaks and boundary-layer ozone enhancements. Particularly, EAC4 exactly captured the SI-induced sub-high ozone layers in the middle troposphere of Changchun (on June 12) and the lower troposphere of Hong Kong (on June 13). This qualitative comparison suggests that EAC4 had a powerful ability to reproduce both the SI dynamics and boundary-layer photochemical processes. The quantitative statistics (Table 1) further reveal that EAC4 ozone reanalysis had the strongest correlation (R = 0.947), the lowest mean absolute bias (MAB = 19.1 ppbv), the lowest root mean square error (RMSE = 36.9 ppbv), and the largest index of agreement (IOA = 0.985) to the ozonesonde observation. The MAB was even comparable to that in specific model studies (Hu et al., 2017; Wang et al., 2022). Overall, this sonde-based validation, along with subsequent validation against with nationwide surface ozone observations (Fig. 4A and Table 1), provides us enough confidence in adopting EAC4 reanalysis to explore the trough-induced stratospheric ozone intrusion on a larger spatial scale.

Table 1. Evaluation statistics for commonly-used ozone products compared with the ozonesondes from Beijing, Changchun, and Hong Kong, and ground-based measurements across 76 cities in China

Variables	R	MAB (ppbv)	RMSE (ppbv)	IOA
O_3-AIRS & O_3-Sonde	0.793	67.2	122.1	0.907
O_3-MERRA2 & O_3-Sonde	0.939	27.3	43.5	0.981
O_3-EAC4 & O_3-Sonde	0.947	19.1	36.9	0.985
O_3-EAC4 & O_3-Ground	0.697	12.4	23.5	0.961

* R, MAB, RMSE, and IOA denote the correlation coefficient, mean absolute bias, root mean square error, and index of agreement, respectively.

Fig. 3 illustrates the EAC4-based three-dimensional structure of high-level trough-induced stratospheric ozone intrusion over China. High ozone concentrations at 200 hPa aligned with the trough location, extending southwestward (June 10) and southward (June 11–13) along the trough axis, which well explained the high-level secondary ozone peaks over Beijing since June 11 and over Changchun on June 13 (Fig. 2A and B). At 400 hPa, the SDI-induced O_3-rich filament and WCB-related O_3-poor belt were distinguishable on each side of the trough axis, elongated approximately 2000 km and 200 km in width. This feature was most prominent on June 11, the day with the strongest stratospheric intrusion. On June 12, the SDI-induced O_3-rich filament at 400 hPa stretched to northeastern China, explaining the observed high ozone laminae in the middle troposphere of Changchun (Fig. 2B). Considering no high-level secondary ozone peak in Changchun on this day, the middle-tropospheric high ozone laminae can be explained as a result of northward advection transport of the pre-intruded O_3-rich stratospheric air in the southern regions. Note that on June 11, the day with the strongest stratospheric intrusion, an O_3-rich filament appeared in the lower troposphere (700 hPa) of southern China, indicating the southern edge of stratospheric intrusion. This O_3-rich filament persisted in subsequent days and be exactly captured by Hong Kong's ozonesonde on June 13 (Fig. 2C). From June 11 to 13, there was a significant northeastward transport and dispersion of O_3-rich filament due to the strengthening southwesterly winds in the lower troposphere of eastern China. Through vertical and horizontal transport, lower tropospheric ozone concentrations increased by approximately 20 ppbv across eastern China, consistent with the 18 ppbv ozone increase observed in 2–6 km height over Beijing, indicating

https://doi.org/10.5194/egusphere-2025-15
Preprint. Discussion started: 31 March 2025

widespread enhancement of lower-tropospheric ozone background due to ongoing stratospheric ozone accumulation.

Compared with total ozone, stratospheric ozone tracer (O_3S) provides a more direct view of stratospheric intrusion (Fig. 3B). The three-dimensional O_3S structure depicts the high-level trough-induced stratospheric ozone intrusion as a sheet-like lowering of the O_3S-rich layer along the western flank of the trough and an O_3S-rich tongue extending southward and westward from the trough base. These features aligned with the typical structure of extratropical stratospheric intrusion associated with tropopause folding (Bithell et al., 1999; Hocking et al., 2007). On June 10, stratospheric intrusion directly hit the Tibetan Plateau, triggering extremely high surface ozone concentrations. From June 11 to 13, the O_3S-rich tongue progressed eastward into eastern China with the trough's eastward movement. Unlike that in the Tibetan Plateau, the O_3S-rich tongue in eastern China penetrated to the lower free troposphere but was then blocked and did not further intrude the surface layer. This result agreed well with the observed high ozone laminae in 3.5–6.0 km height over Hong Kong (Fig. 2C), suggestive of no direct intrusion to the surface in the low-elevation eastern China. Nevertheless, these O_3S-rich stratospheric air masses can be further transported into the atmospheric boundary layer via convective mixing, contributing to boundary layer ozone increase. However, their stratospheric characteristics (high ozone, low humidity) tend to be lost due to strong turbulence mixing, eventually becoming unrecognizable in the atmospheric boundary layer. Interestingly, another stratospheric intrusion induced by severe tropical storm (name: “Yagi”) over the Northwest Pacific provided a parallel reference (Fig. 3B). Compared with the tropical storm-induced stratospheric instruction, the high-level trough-induced stratospheric intrusion descended to a lower altitude, causing widespread O_3S signals in the atmospheric boundary layer over eastern China.

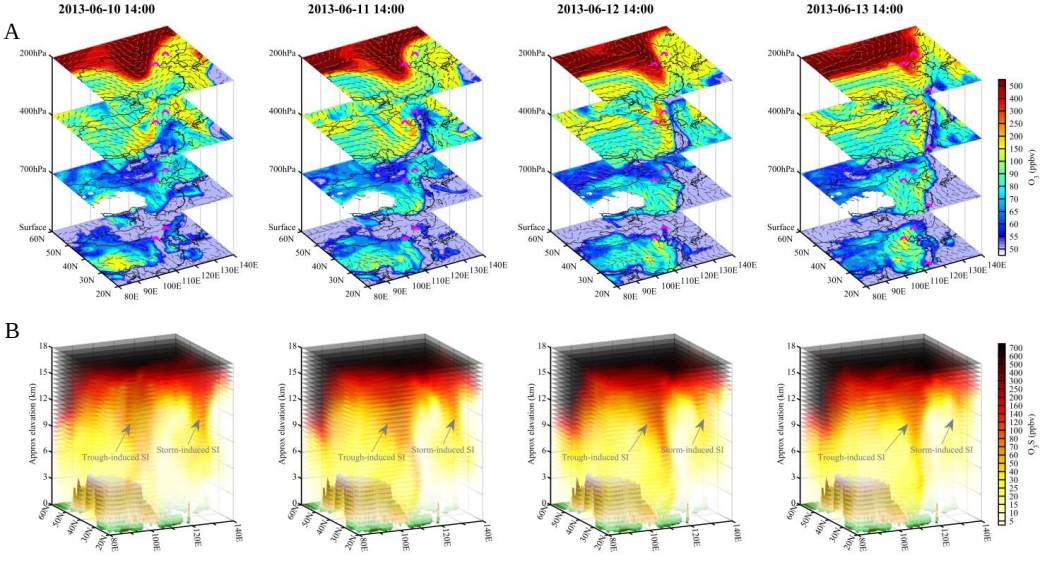

Fig. 3. (A) Spatial distribution of ozone concentrations in 200, 400, 700 hPa, and surface layer. (B) Three-dimensional structure of stratospheric ozone tracer concentrations. Magenta half-circles mark the locations of ozonesondes at different sites (Beijing, Changchun and Hong Kong) on different days.

3.3 Stratospheric intrusion contribution to surface ozone pollution

Fig. 4A presents the spatial distribution of surface ozone concentrations derived from ground-based measurements

https://doi.org/10.5194/egusphere-2025-15
Preprint. Discussion started: 31 March 2025

and EAC4 reanalysis during the SI event. The EAC4-based surface ozone reanalysis agreed well with nationwide ground-based observations (R = 0.697, MAB = 12.4 ppbv, RMSE = 23.5 ppbv, and IOA = 0.961), confirming the reliability of the EAC4 reanalysis again as the previous validation with ozonesondes. On June 10, the Tibetan Plateau experienced high ozone concentrations near or exceeding 80 ppbv, with observed ozone in Lhasa reaching up to 100 ppbv at 14:00 BJT. In contrast, eastern China exhibited low ozone concentrations (< 40 ppbv) due to cloudy and rainy weather on this day. From June 10 to 13, surface ozone concentrations decreased day by day in the Tibetan Plateau, while they increased from west to east in eastern China. By June 13, eastern China suffered severe ozone pollution, with observed ozone concentrations exceeding 100 ppbv in most of the NCP cities. From June 10 to 13, the continuous stratospheric dry intrusion led to a weather transition from cloudy to cloudless in eastern China (Fig. 1B), enhancing photochemical ozone production due to the abundance of ozone precursors over there. Strong solar radiation in cloudless weather also promoted the development of thermal convection, facilitating the mixing of O_3-rich stratospheric air from the free troposphere into the surface layer. These two mechanisms combined to trigger severe ozone pollution in eastern China on June 13. The continue ozonesondes in Beijing provide convincing evidence for these two mechanisms. Returning to Fig. 2A, boundary-layer ozone concentrations in Beijing increased significantly from 57.8 ppbv on June 10 to 120.6 ppbv on June 13. Considering the sharp ozone gradient in the interface between the atmospheric boundary layer and the lower free troposphere, the dramatic increase in boundary-layer ozone can be primarily attributed to photochemical production (Liao et al., 2024). However, the concurrent rise in ozone concentrations in the lower free troposphere (an 18 ppbv ozone increase in 2–6 km height from June 10 to 13) indicated that stratospheric ozone intrusion contributed to elevating lower-tropospheric ozone background, ultimately exacerbating boundary layer ozone pollution.

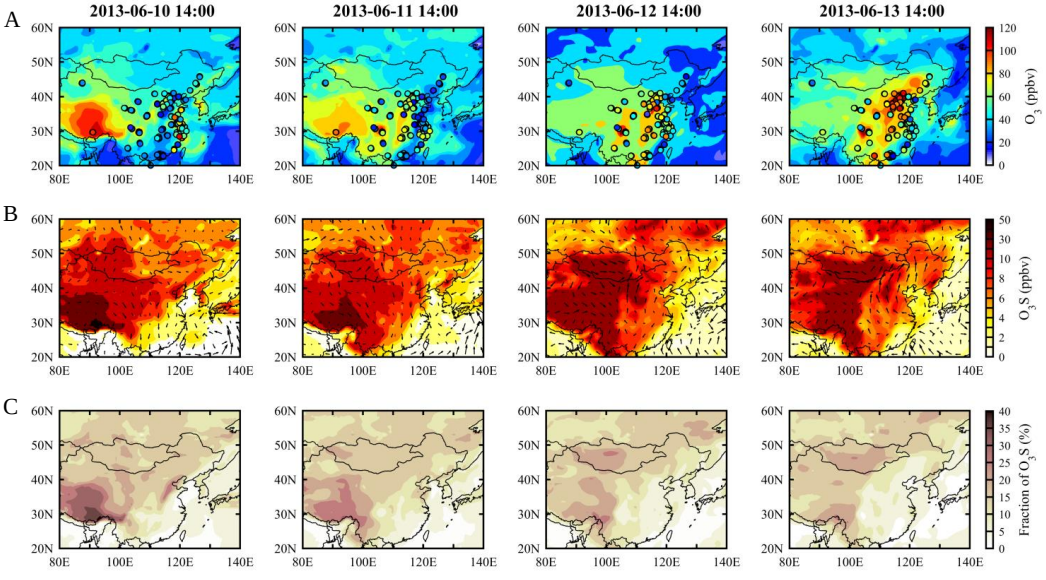

Fig. 4. (A) Surface spatial distribution of total ozone concentration derived from ground-based measurement (dots) and EAC4 reanalysis (shading). (B) Surface spatial distribution of stratospheric ozone tracer concentration derived from EAC4 reanalysis. (C) Surface spatial distribution of stratospheric ozone tracer fraction in total ozone calculated from EAC reanalysis.

To quantify the contribution of stratospheric ozone intrusion to surface ozone pollution, Fig. 4B illustrates the

https://doi.org/10.5194/egusphere-2025-15
Preprint. Discussion started: 31 March 2025

surface spatial distribution of EAC4-based stratospheric ozone tracer (O_3S) concentrations during the SI event, and Fig. 4C shows the fraction of O_3S in surface ozone. The high-elevation Tibetan Plateau received high-concentration ozone from stratospheric intrusion, particularly on June 10 when the upper-level trough was oriented northeast-southwest towards the Tibetan Plateau. On this day, surface O_3S cocnentration exceeded 30 ppbv (up to 48.5 ppbv) in the Tibetan Plateau, contributing to over 30 % of the surface ozone concentration (up to 44.7 %). Subsequent days saw a gradual decrease in O_3S over the Tibetan Plateau as it was dispersed eastward and then northward to the Mongolian Plateau. On June 12 and 13, significant O_3S hotspots (> 20 ppbv) appeared in the Mongolian Plateau. In conjunction with the observed ozone profiles in Beijing (Fig. 2A) and the three-dimensional O_3S structure (Fig. 3B), the elevated O_3S concentrations in the Mongolian Plateau can be attributed to wind-driven dispersion of the intruded O_3-rich stratospheric air rather than direct stratospheric intrusion at the local scale. Here, the intruded O_3-rich stratospheric air included the "aged" stratospheric air pre-intruded in the Tibetan Plateau and the "fresh" stratospheric air in the O_3S-rich tongue over eastern China. Due to continuous intrusion and accumulation, surface O_3S concentrations also increased in eastern China, whereas their fraction in surface ozone decreased as local ozone photochemical production accelerated in the sunny weather. On June 13, surface O_3S concentrations in eastern China ranged from 3 to 15 ppbv, accounting for 2–10 % of surface ozone concentrations. Two O_3S hotspots were identified in eastern China: one in the Taihang Mountains (10–15 ppbv) and another in southern NCP (8–10 ppbv). In the highly polluted NCP region, O_3S accounted for approximately 10 % of surface ozone concentrations, significantly lower than the proportion in the Tibetan Plateau.

4 Conclusions and Discussion

This study reveals that the high-level trough-induced stratospheric ozone intrusion over China did not occur as a local-scale vertical descent from the stratosphere to the lower troposphere just at the mid-latitude location where tropopause folding occurs; instead, it involved a long-range transport from mid-latitude tropopause folding zone (e.g., Beijing) to lower-latitude areas (e.g., Hong Kong), featuring an O_3-rich "tongue" structure with high-level secondary ozone peak at the base of tongue (e.g., over Beijing) and lower-tropospheric sub-high ozone layer at the tip of tongue (e.g., over Hong Kong). The O_3-rich "tongue" swept through the high-elevation Tibetan Plateau when the high-level trough extended towards this highland region at its initial stage, triggering extreme surface ozone pollution. With the eastward movement of high-level trough, the O_3-rich "tongue" penetrated into the lower troposphere of low-elevation eastern China. Over there, the intruded O_3-rich stratospheric air masses in the lower troposphere, including the "aged" stratospheric air horizontally transported from the Tibetan Plateau and the "fresh" stratospheric air vertically transported from O_3-rich "tongue", were then entrained into the atmospheric boundary layer via lower-tropospheric dynamic processes (e.g. subsidence motion and convective mixing). At the same time, the strengthening lower-tropospheric southwesterly winds with the eastward movement of high-level trough gradually participated to transport these O_3-rich stratospheric air back to the mid-latitudes, ultimately exacerbating surface ozone pollution in the NCP region (e.g., Beijing). While several SI events have been reported in China (Chang et al., 2023; Hong et al., 2024; Li et al., 2015; Luo et al., 2024; Wang et al., 2020a; Zhang et al., 2022; Zhao et al., 2024), this trough-induced SI episode may be the first event of its widespread impact and refined structure documented (Fig. 5).

The quantitative stratospheric intrusion contributions derived from the fully-validated EAC4 reanalysis are generally consistent with previous model results in China. In the low-elevation eastern China, surface O_3S concentrations were previously estimated to be in the range of 5–20 ppbv during the SI events (Wang et al., 2020a; Zhang et al., 2022; Chang et al., 2023). Our EAC4-based estimation agreed well with this range, reflecting the typical magnitude of SI contribution in the low-elevation eastern China. As for the high-elevation Tibetan Plateau, a

https://doi.org/10.5194/egusphere-2025-15
Preprint. Discussion started: 31 March 2025

case-based model study (Skerlak et al., 2019) revealed that stratospheric tracer concentrations at the surface reach peak values of 20 % of the imposed stratospheric value, and a month-based model study (Yin et al., 2023) suggested that 36.5 % of surface ozone in the hotspot of the southern Tibetan Plateau was contributed by stratospheric ozone intrusion. Our EAC4-based estimation was comparable to these fractional contributions, corroborating the potential of SI to significantly influence surface ozone concentrations in this highland region. Besides, ground-based stratospheric tracer method had been developed to quantify the stratospheric intrusion contribution over China. While Chen et al. (2024) identified the nationwide SI-induced ozone enhancement as a west-low-east-high spatial distribution pattern based on surface ozone and carbon monoxide observations, Lin et al. (2021) determined a west-high-east-low spatial distribution pattern of SI-induced ozone contribution based on ground-based cosmogenic ^{35}S observations at the Himalayas and beyond. Our fully-validated result appears to support the latter, which conforms to the common knowledge that the highland regions are more susceptible to stratospheric intrusion because of their proximity to the stratosphere (Skerlak et al., 2019; Wang et al., 2020b; Lin et al., 2021).

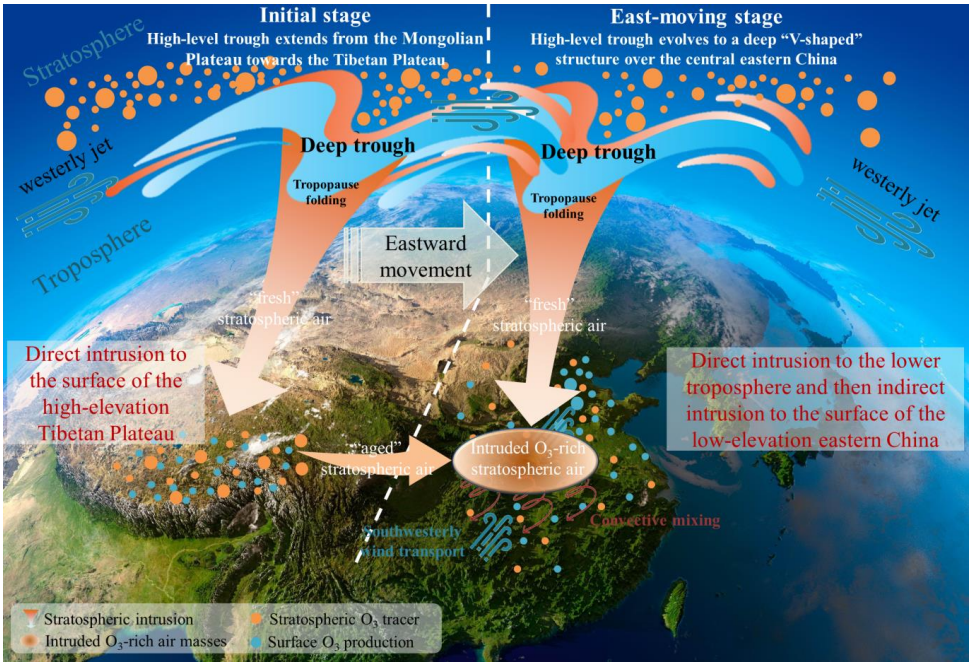

Fig. 5. Schematic illustration of high-level trough-induced stratospheric ozone intrusion influence on surface ozone pollution over China

To the best of our knowledge, this study is the first to utilize continuous and multi-site ozonesondes to investigate stratospheric ozone intrusion. While we acknowledge that a single case study may not be fully representative, it effectively demonstrates the value of continuous and multi-site ozonesonde measurements in enhancing our understanding of stratospheric ozone intrusion phenomena. On the other hand, these continuous and multi-site ozonesondes provide a valuable and unique benchmark for examining the capacity of those commonly-used ozone products (including AIRS satellite observation, MERRA2 and EAC4 ozone reanalysis) in characterizing stratospheric ozone intrusion. Previous study indicated that MERRA2 can be used in scientific studies to identify SIs by both atmospheric dynamics and composition (Knowland et al., 2017). Here, we demonstrate that EAC4, a

https://doi.org/10.5194/egusphere-2025-15
Preprint. Discussion started: 31 March 2025

publicly available dataset from European Centre for Medium-Range Weather Forecasts, performs better than MERRA2 in quantitatively characterizing stratospheric ozone intrusion via comparative evaluation. Moreover, in contrast to MERRA2, EAC4 simulates full ozone chemistry in the troposphere (an extended version of the Carbon Bond 2005 (CB05) chemical mechanism), allowing to determine the influence of stratospheric ozone on surface concentrations separate from photochemically produced ozone. Therefore, this is a proof opening the door to detailed multiyear analyses of stratospheric ozone intrusion and their quantitative contribution to surface ozone over China and worldwide based on the publicly available EAC4 ozone reanalysis.

Data availability. All used data, excluding the ozonesonde in Beijing and Changchun, are open source. ERA5 atmospheric data are available from Copernicus Climate Change Service (C3S) Climate Data Store accessible at https://cds.climate.copernicus.eu/. EAC4 ozone reanalysis were obtained from Copernicus Atmospheric Monitoring Service Data Store accessible at https://ads.atmosphere.copernicus.eu/. The MODIS true color images are available from the NASA Earth Observations (NEO): https://neo.gsfc.nasa.gov/. The AIRS and MERRA2 ozone products were obtained from Goddard Earth Sciences Data and Information Services Center accessible at https://disc.gsfc.nasa.gov/. The ozonesonde data in Hong Kong were obtained from World Ozone and Ultraviolet Radiation Data Centre accessible at https://woudc.org/. The ozonesonde data in Beijing and Changchun are available from the first author upon reasonable request (zhliao@ium.cn).

Author contributions

Z.L. conceived the original idea, analyzed the data, and wrote the first version manuscript. J.Z. designed intensive ozonesonde experiments in Beijing and Changchun. Z.M supervised the research project. All authors discussed the results and commented on the manuscript.

Competing interests

The authors declare no competing interests.

Acknowledgements

This research has been supported by the National Natural Science Foundation of China (Grant Nos. 42405115, 42293321 and 42207115).

References

Akritidis, D., Katragkou, E., Zanis, P., Pytharoulis, I., Melas, D., Flemming, J., Inness, A., Clark, H., Plu, M., and Eskes, H.: A deep stratosphere-to-troposphere ozone transport event over Europe simulated in CAMS global and regional forecast systems: analysis and evaluation, Atmos Chem Phys, 18, 15515-15534, 10.5194/acp-18-15515-2018, 2018.

Appenzeller, C. and Davies, H. C.: Structure of stratospheric intrusions into the troposphere, Nature, 358, 570-572, 10.1038/358570a0, 1992.

Bartusek, S., Wu, Y. T., Ting, M. F., Zheng, C., Fiore, A., Sprenger, M., and Flemming, J.: Higher-Resolution Tropopause Folding Accounts for More Stratospheric Ozone Intrusions, Geophys Res Lett, 50, ARTN e2022GL101690 10.1029/2022GL101690, 2023.

Bithell, M., Gray, L. J., and Cox, B. D.: A Three-Dimensional View of the Evolution of Midlatitude Stratospheric Intrusions, Journal of the Atmospheric Sciences, 56, 673-688, https://doi.org/10.1175/1520-0469(1999)056<0673:ATDVOT>2.0.CO;2, 1999.

Browning, K. A.: The dry intrusion perspective of extra-tropical cyclone development, Meteorological Applications, 4, 317-324, https://doi.org/10.1017/S1350482797000613, 1997.

https://doi.org/10.5194/egusphere-2025-15
Preprint. Discussion started: 31 March 2025

377 Browning, K. A. and Roberts, N. M.: Structure of a frontal cyclone, Q J Roy Meteor Soc, 120, 1535-1557,
378 https://doi.org/10.1002/qj.49712052006, 1994.
379 Chang, F. Y., Li, J. D., Li, N., and Liao, H.: Stratospheric intrusion may aggravate widespread ozone pollution through both
380 vertical and horizontal advections in eastern China during summer, Front Env Sci-Switz, 10, Artn 1115746
381 10.3389/Fenvs.2022.1115746, 2023.
382 Chen, X. L., Ma, Y. M., Kelder, H., Su, Z., and Yang, K.: On the behaviour of the tropopause folding events over the
383 Tibetan Plateau, Atmos Chem Phys, 11, 5113-5122, 10.5194/acp-11-5113-2011, 2011.
384 Chen, Z., Liu, J., Qie, X., Cheng, X., Yang, M., Shu, L., and Zang, Z.: Stratospheric influence on surface ozone pollution in
385 China, Nat Commun, 15, 4064, 10.1038/s41467-024-48406-x, 2024.
386 Chen, Z. X., Liu, J. E., Cheng, X. G., Yang, M. M., and Shu, L.: Stratospheric influences on surface ozone increase during
387 the COVID-19 lockdown over northern China, Npj Clim Atmos Sci, 6, Artn 76
388 10.1038/S41612-023-00406-2, 2023.
389 Cristofanelli, P., Bracci, A., Sprenger, M., Marinoni, A., Bonafè, U., Calzolari, F., Duchi, R., Laj, P., Pichon, J. M., Roccato, F.,
390 Venzac, H., Vuillermoz, E., and Bonasoni, P.: Tropospheric ozone variations at the Nepal Climate Observatory-Pyramid
391 (Himalayas, 5079 m a.s.l.) and influence of deep stratospheric intrusion events, Atmos Chem Phys, 10, 6537-6549,
392 10.5194/acp-10-6537-2010, 2010.
393 Dreessen, J.: A Sea Level Stratospheric Ozone Intrusion Event Induced within a Thunderstorm Gust Front, B Am
394 Meteorol Soc, 100, 1259-1275, 10.1175/Bams-D-18-0113.1, 2019.
395 Hersbach, H., Bell, B., Berrisford, P., Hirahara, S., Horányi, A., Muñoz-Sabater, J., Nicolas, J., Peubey, C., Radu, R.,
396 Schepers, D., Simmons, A., Soci, C., Abdalla, S., Abellan, X., Balsamo, G., Bechtold, P., Biavati, G., Bidlot, J., Bonavita, M.,
397 De Chiara, G., Dahlgren, P., Dee, D., Diamantakis, M., Dragani, R., Flemming, J., Forbes, R., Fuentes, M., Geer, A.,
398 Haimberger, L., Healy, S., Hogan, R. J., Hólm, E., Janisková, M., Keeley, S., Laloyaux, P., Lopez, P., Lupu, C., Radnoti, G., de
399 Rosnay, P., Rozum, I., Vamborg, F., Villaume, S., and Thépaut, J. N.: The ERA5 global reanalysis, Q J Roy Meteor Soc, 146,
400 1999-2049, 10.1002/qj.3803, 2020.
401 Hocking, W. K., Carey-Smith, T., Tarasick, D. W., Argall, P. S., Strong, K., Rochon, Y., Zawadzki, I., and Taylor, P. A.:
402 Detection of stratospheric ozone intrusions by windprofiler radars, Nature, 450, 281-284, 10.1038/nature06312, 2007.
403 Hong, J., Wang, H., Wang, W., Zhu, J., Deng, H., and Wang, H.: Impacts of stratosphere-to-troposphere transport on
404 tropospheric ozone in southeastern China: insights from ozonesonde observations, Environ Res Lett, 19, 064068,
405 10.1088/1748-9326/ad4ef9, 2024.
406 Hu, L., Jacob, D. J., Liu, X., Zhang, Y., Zhang, L., Kim, P. S., Sulprizio, M. P., and Yantosca, R. M.: Global budget of
407 tropospheric ozone: Evaluating recent model advances with satellite (OMI), aircraft (IAGOS), and ozonesonde
408 observations, Atmos Environ, 167, 323-334, 10.1016/j.atmosenv.2017.08.036, 2017.
409 Hwang, S. H., Kim, J., and Cho, G. R.: Observation of secondary ozone peaks near the tropopause over the Korean
410 peninsula associated with stratosphere-troposphere exchange, J Geophys Res-Atmos, 112, Artn D16305
411 10.1029/2006jd007978, 2007.
412 Inness, A., Ades, M., Agusti-Panareda, A., Barré, J., Benedictow, A., Blechschmidt, A. M., Dominguez, J. J., Engelen, R.,
413 Eskes, H., Flemming, J., Huijnen, V., Jones, L., Kipling, Z., Massart, S., Parrington, M., Pench, V. H., Razinger, M., Remy, S.,
414 Schulz, M., and Suttie, M.: The CAMS reanalysis of atmospheric composition, Atmos Chem Phys, 19, 3515-3556,
415 10.5194/acp-19-3515-2019, 2019.
416 Knowland, K. E., Ott, L. E., Duncan, B. N., and Wargan, K.: Stratospheric Intrusion-Influenced Ozone Air Quality
417 Exceedances Investigated in the NASA MERRA-2 Reanalysis, Geophys Res Lett, 44, 10691-10701,
418 10.1002/2017GL074532, 2017.
419 Langford, A. O., Brioude, J., Cooper, O. R., Senff, C. J., Alvarez, R. J., Hardesty, R. M., Johnson, B. J., and Oltmans, S. J.:
420 Stratospheric influence on surface ozone in the Los Angeles area during late spring and early summer of 2010, J

https://doi.org/10.5194/egusphere-2025-15
Preprint. Discussion started: 31 March 2025

Geophys Res-Atmos, 117, Artn D00v06
10.1029/2011jd016766, 2012.
Lemoine, R.: Secondary maxima in ozone profiles, Atmos Chem Phys, 4, 1085-1096, DOI 10.5194/acp-4-1085-2004, 2004.
Li, D., Bian, J. C., and Fan, Q. J.: A deep stratospheric intrusion associated with an intense cut-off low event over East Asia, Sci China Earth Sci, 58, 116-128, 10.1007/s11430-014-4977-2, 2015.
Liao, Z., Gao, M., Zhang, J., Sun, J., Quan, J., Jia, X., Pan, Y., and Fan, S.: Mixing-layer-height-referenced ozone vertical distribution in the lower troposphere of Chinese megacities: stratification, classification, and meteorological and photochemical mechanisms, Atmos. Chem. Phys., 24, 3541-3557, 10.5194/acp-24-3541-2024, 2024.
Lin, M., Su, L., Shaheen, R., Fung, J. C. H., and Thiemens, M. H.: Detection of deep stratospheric intrusions by cosmogenic ^{35}S, P Natl Acad Sci USA, 113, 11131-11136, 10.1073/pnas.1609919113, 2016.
Lin, M., Wang, K., Kang, S., Li, Y., Fan, Z., and Thiemens, M. H.: Isotopic signatures of stratospheric air at the Himalayas and beyond, Sci Bull, 66, 323-326, https://doi.org/10.1016/j.scib.2020.11.005, 2021.
Lin, M. Y., Fiore, A. M., Horowitz, L. W., Langford, A. O., Oltmans, S. J., Tarasick, D., and Rieder, H. E.: Climate variability modulates western US ozone air quality in spring via deep stratospheric intrusions, Nat Commun, 6, Artn 7105
10.1038/Ncomms8105, 2015.
Liu, X., Fu, Y., Zhang, L., Li, H., Burr, G. S., Bi, Y., and Zhao, G.: Deep stratospheric intrusion events in China revealed on the ground by cosmogenic 10Be/7Be, Communications Earth & Environment, 5, 553, 10.1038/s43247-024-01727-7, 2024.
Lu, X., Zhang, L., Chen, Y. F., Zhou, M., Zheng, B., Li, K., Liu, Y. M., Lin, J. T., Fu, T. M., and Zhang, Q.: Exploring 2016-2017 surface ozone pollution over China: source contributions and meteorological influences, Atmos Chem Phys, 19, 8339-8361, 10.5194/acp-19-8339-2019, 2019.
Luo, Y., Zhao, T., Meng, K., Hu, J., Yang, Q., Bai, Y., Yang, K., Fu, W., Tan, C., Zhang, Y., Zhang, Y., and Li, Z.: A mechanism of stratospheric O3 intrusion into the atmospheric environment: a case study of the North China Plain, Atmos. Chem. Phys., 24, 7013-7026, 10.5194/acp-24-7013-2024, 2024.
Meng, K., Zhao, T., Bai, Y., Wu, M., Cao, L., Hou, X., Luo, Y., and Jiang, Y.: Tracing the origins of stratospheric ozone intrusions: direct vs. indirect pathways and their impacts on Central and Eastern China in spring–summer 2019, Atmos. Chem. Phys., 24, 12623-12642, 10.5194/acp-24-12623-2024, 2024.
Monks, P. S., Archibald, A. T., Colette, A., Cooper, O., Coyle, M., Derwent, R., Fowler, D., Granier, C., Law, K. S., Mills, G. E., Stevenson, D. S., Tarasova, O., Thouret, V., von Schneidemesser, E., Sommariva, R., Wild, O., and Williams, M. L.: Tropospheric ozone and its precursors from the urban to the global scale from air quality to short-lived climate forcer, Atmos Chem Phys, 15, 8889-8973, 10.5194/acp-15-8889-2015, 2015.
Ojha, N., Pozzer, A., Akritidis, D., and Lelieveld, J.: Secondary ozone peaks in the troposphere over the Himalayas, Atmos Chem Phys, 17, 6743-6757, 10.5194/acp-17-6743-2017, 2017.
Ou-Yang, C. F., Babu, S. R., Lee, J. R., Yen, M. C., Griffith, S. M., Lin, C. C., Chang, S. C., and Lin, N. H.: Detection of stratospheric intrusion events and their role in ozone enhancement at a mountain background site in sub-tropical East Asia, Atmos Environ, 268, ARTN 118779
10.1016/j.atmosenv.2021.118779, 2022.
Skerlak, B., Pfahl, S., Sprenger, M., and Wernli, H.: A numerical process study on the rapid transport of stratospheric air down to the surface over western North America and the Tibetan Plateau, Atmos Chem Phys, 19, 6535-6549, 10.5194/acp-19-6535-2019, 2019.
Stohl, A., Bonasoni, P., Cristofanelli, P., Collins, W., Feichter, J., Frank, A., Forster, C., Gerasopoulos, E., Gäggeler, H., James, P., Kentarchos, T., Kromp-Kolb, H., Krüger, B., Land, C., Meloen, J., Papayannis, A., Priller, A., Seibert, P., Sprenger, M., Roelofs, G. J., Scheel, H. E., Schnabel, C., Siegmund, P., Tobler, L., Trickl, T., Wernli, H., Wirth, V., Zanis, P., and Zerefos, C.:

https://doi.org/10.5194/egusphere-2025-15
Preprint. Discussion started: 31 March 2025

Stratosphere-troposphere exchange: A review, and what we have learned from STACCATO, J Geophys Res-Atmos, 108, Artn 8516
10.1029/2002jd002490, 2003.
Trickl, T., Bärtsch-Ritter, N., Eisele, H., Furger, M., Mücke, R., Sprenger, M., and Stohl, A.: High-ozone layers in the middle and upper troposphere above Central Europe: potential import from the stratosphere along the subtropical jet stream, Atmos Chem Phys, 11, 9343-9366, 10.5194/acp-11-9343-2011, 2011.
Wang, H. L., Lu, X., Jacob, D. J., Cooper, O. R., Chang, K. L., Li, K., Gao, M., Liu, Y. M., Sheng, B. S., Wu, K., Wu, T. W., Zhang, J., Sauvage, B., Nédélec, P., Blot, R., and Fan, S. J.: Global tropospheric ozone trends, attributions, and radiative impacts in 1995-2017: an integrated analysis using aircraft (IAGOS) observations, ozonesonde, and multi-decadal chemical model simulations, Atmos Chem Phys, 22, 13753-13782, 10.5194/acp-22-13753-2022, 2022.
Wang, H. Y., Wang, W., Huang, X., and Ding, A. J.: Impacts of stratosphere-to-troposphere-transport on summertime surface ozone over eastern China, Sci Bull, 65, 276-279, 10.1016/j.scib.2019.11.017, 2020a.
Wang, X. Y., Wu, Y. T., Randel, W., and Tilmes, S.: Stratospheric contribution to the summertime high surface ozone events over the western united states, Environ Res Lett, 15, ARTN 1040a6
10.1088/1748-9326/abba53, 2020b.
Yang, J., Wang, K., Lin, M., Yin, X., and Kang, S.: Not biomass burning but stratospheric intrusion dominating tropospheric ozone over the Tibetan Plateau, Proc Natl Acad Sci U S A, 119, e2211002119, 10.1073/pnas.2211002119, 2022.
Yates, E. L., Iraci, L. T., Roby, M. C., Pierce, R. B., Johnson, M. S., Reddy, P. J., Tadic, J. M., Loewenstein, M., and Gore, W.: Airborne observations and modeling of springtime stratosphere-to-troposphere transport over California, Atmos Chem Phys, 13, 12481-12494, 10.5194/acp-13-12481-2013, 2013.
Yin, X. F., Rupakheti, D., Zhang, G. S., Luo, J. L., Kang, S. C., de Foy, B., Yang, J. H., Ji, Z. M., Cong, Z. Y., Rupakheti, M., Li, P., Hu, Y. L., and Zhang, Q. G.: Surface ozone over the Tibetan Plateau controlled by stratospheric intrusion, Atmos Chem Phys, 23, 10137-10143, 10.5194/acp-23-10137-2023, 2023.
Zhang, J.-q., Xuan, Y., Xia, X.-A., Liu, M., Yan, X.-l., Pang, L., Bai, Z.-X., and Wang, X.: Performance Evaluation of a Self-Developed Ozonesonde and Its Application in an Intensive Observational Campaign, Atmospheric and Oceanic Science Letters, 7, 175 - 179, 2013.
Zhang, J. Q., Li, D., Bian, J. C., Xuan, Y. J., Chen, H. B., Bai, Z. X., Wan, X. W., Zheng, X. D., Xia, X. G., and Lü, D. R.: Long-term ozone variability in the vertical structure and integrated column over the North China Plain: results based on ozonesonde and Dobson measurements during 2001-2019, Environ Res Lett, 16, Artn 074053
10.1088/1748-9326/Ac109f, 2021.
Zhang, Y. J., Li, J., Yang, W. Y., Du, H. Y., Tang, X., Ye, Q., Wang, Z. X., Sun, Y. L., Pan, X. L., Zhu, L. L., and Wang, Z. F.: Influences of stratospheric intrusions to high summer surface ozone over a heavily industrialized region in northern China, Environ Res Lett, 17, Artn 094023
10.1088/1748-9326/Ac8b24, 2022.
Zhao, K., Chen, Y., Lian, P., Li, W., Yang, F., Zhang, X., and Yang, R.: Impact of stratospheric intrusions on surface ozone enhancement in Hong Kong in the lower troposphere: Implications for ozone control strategy, Atmos Environ, 329, 120539, https://doi.org/10.1016/j.atmosenv.2024.120539, 2024.
Zhao, K. H., Huang, J. P., Wu, Y. H., Yuan, Z. B., Wang, Y. W., Li, Y., Ma, X. D., Liu, X. H., Ma, W., Wang, Y., and Zhang, X. Y.: Impact of Stratospheric Intrusions on Ozone Enhancement in the Lower Troposphere and Implication to Air Quality in Hong Kong and Other South China Regions, J Geophys Res-Atmos, 126, ARTN e2020JD033955
10.1029/2020JD033955, 2021.
Zheng, X., Yang, W., Sun, Y., Geng, C., Liu, Y., and Xu, X.: Comment on “Transport of substantial stratospheric ozone to the surface by a dying typhoon and shallow convection” by Chen et al. (2022), Atmos. Chem. Phys., 24, 3759-3768,

https://doi.org/10.5194/egusphere-2025-15
Preprint. Discussion started: 31 March 2025

509 10.5194/acp-24-3759-2024, 2024.
510 Zhu, F., Luo, J., Wang, Z., Jin, H., Zhao, Q., Wang, Z., Luo, F., and Gu, M.: The Impact of Stratosphere-to-Troposphere
511 Transport Associated with the Northeast China Cold Vortex on Surface Ozone Concentrations in Eastern China, Journal
512 of Applied Meteorology and Climatology, https://doi.org/10.1175/JAMC-D-24-0027.1, 2024.
513